

# VALIDATION OF THE PERFORMANCE OF A HIGH-ACCURACY COMPACT INTERFEROMETRIC SENSOR

Vivek G. Badami and Colin D. Fletcher  
Zygo Corporation  
Middlefield, CT, USA

## INTRODUCTION

This paper describes the metrology for the validation of displacement measurement performance of a new high-accuracy, multi-channel, fiber-based, low drift, absolute distance measuring interferometric sensor system. The system was designed for demanding applications requiring thermally passive, electrically immune, compact sensors with an extremely long mean time between failure (MTBF).

Although the system is capable of displacement and absolute distance measurement, the main focus of this paper is the metrology used to validate the latter. The performance of the system under test (SUT) is compared to a modified commercial displacement measuring interferometer (DMI) system (Zygo ZMI 4000). Uncertainty contributors in the validation metrology (VM) system are minimized through a compact metrology loop and compensation of Abbè errors. The design of the validation metrology is driven by a comprehensive uncertainty budget, with resulting displacement uncertainties ( $k=2$ ) at the part per million (ppm) level. A detailed description of the setup and uncertainty budget is provided.

## THE SYSTEM UNDER TEST (SUT)

The system under test is described in detail in these proceedings and elsewhere [1]. The system is designed to operate over a range of  $\pm 250 \mu\text{m}$  at a standoff of 1.2 mm. It operates at near-IR ( $\sim 1550 \text{ nm}$ ) wavelengths and has sub-nanometer resolution.

## VALIDATION METROLOGY

The displacement measurement performance of the displacement sensor under test is validated by comparison to a modified commercial DMI. In order to effectively validate the performance of the SUT, a VM method with commensurate measurement uncertainty is required.

## The Setup

A schematic of the VM setup is shown in Figure 1.

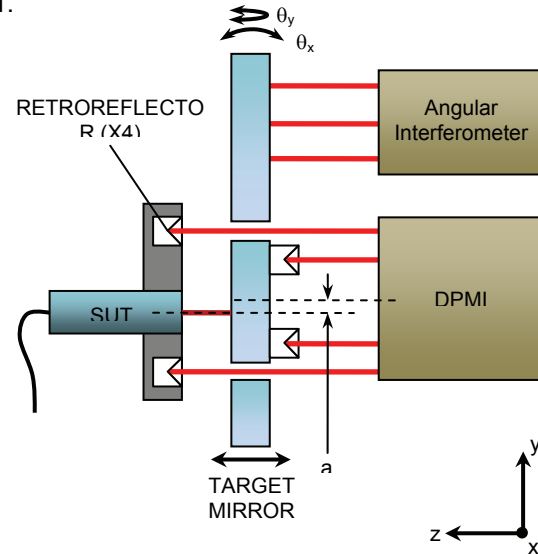


FIGURE 1. Schematic of validation metrology setup.

The heart of the system is a target mirror the displacement of which is measured by both the SUT and the VM. The VM is implemented as a modified differential plane mirror interferometer (DPMI) configuration (Zygo 6191-0188-02) that performs a differential measurement between the target mirror and the mount of the SUT. The beams that probe the mount of the SUT pass through holes in the target mirror. This configuration differs from the standard DPMI configuration in that the plane mirror target on the SUT mount has been replaced by retroreflectors to eliminate any adjustments between the SUT and its mount which could compromise stability. The retroreflectors allow the SUT orientation to be adjusted to orient it normal to the target without compromising alignment of the VM. In addition, retroreflectors on the back of the target mirror also allow for tilting the target mirror to facilitate testing of sensor performance in the presence of mirror tilt. While the figure gives the appearance that the measurement and reference beams of the DPMI are coplanar, in reality, the two beam pairs are

in two mutually orthogonal planes. The reference beams (the ones that pass through the target mirror) are in a plane normal to the plane of the paper, while the measurement beams (the ones that are reflected from the back of the target) are in the plane of the paper. This particular arrangement of beams requires the DPMI to be rotated 45 degrees (about an axis parallel to the beam axis) relative to its standard mounting configuration, resulting in a non-standard mounting configuration. Also, since this interferometer is a polarization based device, the incoming polarization states have to be rotated in order to launch correctly oriented polarization states into the interferometer. The DPMI measures the average of the change in optical path length (OPL) in the two legs of the measurement or reference beam. In other words, the effective point of measurement is midway between the beams, and must be arranged such that this point coincides with the location at which the displacement is to be measured. A second interferometer (Zygo 6191-0624-01) system capable of measuring angular motions of the target mirror is used in tandem with the DPMI to measure the angular motions ( $\theta_x$  and  $\theta_y$ ) of the mirror. This information is used to correct for contributions due to the Abbè offset ( $a$  in Figure 1). The target mirror is coated on one side to provide a reflecting surface for the angular interferometer. The other side (closest to the SUT) is an uncoated bare glass surface that simulates the typical target for the SUT.

### The Measurand

The ultimate goal of the measurement is to determine the fidelity with which the SUT measures the relative displacement between the SUT (specifically the reference surface of the SUT) and target mirror. In order to make this determination, an independent measurement of this displacement is required. The required level of performance is achieved by careful analysis of the metrology loops (see Figure 2).

While a direct measurement of the target mirror relative to reference surface of the VM would provide the ideal metrology, practical considerations result in a more indirect measurement, i.e., between retroreflectors mounted in the mount for the SUT and the rear surface of the target mirror.

The advantages of the differential nature of the measurement may best be understood by

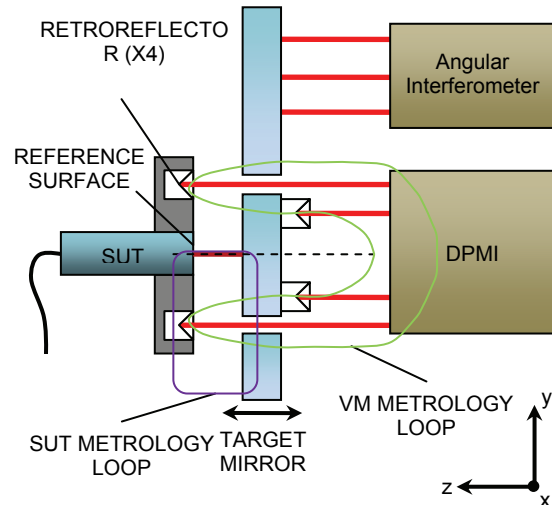


**FIGURE 2. Metrology loops for VM and SUT.**

contrasting this arrangement to a more conventional “back-to-back” arrangement that is used to compare displacement sensors and in particular interferometric sensors. In such a setup the two sensors monitor the displacement of a common target from opposite sides. In this arrangement, the frame that connects the references of the two sensors (beamsplitters in the case conventional interferometers) is part of the metrology loop and any changes in the dimensions of this frame are indistinguishable from the measurand. Thus, thermal effects and vibrations in general become part of the measurement and are not common to the measurement made by both sensors. In contrast to the arrangement described above, the arrangement described here excludes the structure joining the two sensor from the metrology loop in such a manner that virtually all of the rigid-body motions of the mechanical support structure, the target mirror and the mount of the SUT become part of the displacement measured by both sensors, allowing for a more faithful comparison. For instance, motion of the SUT mount is measured by both sensors and affects both measurements equally. The metrology loops and the structural loops are largely decoupled, with most of the supporting staging and hardware being outside the metrology loop. Angular motions are also completely rejected in the absence of an Abbè offset. However, since the Abbè offset cannot be entirely eliminated, a compensation scheme based on the measurement of the rigid-body rotations by another interferometer is used to correct for any residual Abbè offset

contributions. This compensation is discussed in detail below.

While this arrangement provides a relatively compact metrology loop, the contribution of every component within the loop must be estimated and included in the estimate of the measurement uncertainty. Thermal changes in the dimensions of the mount, instabilities in the mounting of the reflectors, etc. are in principle within the metrology loop, although in practice the good temperature control over the short duration of the measurement (typically a few seconds) and the use of low expansion materials, result in negligible uncertainty contributions. For example, the effect of target mirror expansion (which is within the metrology loop) is minimized through use of a low expansion material (fused silica) and stringent temperature control ( $\sim 10$  mK). The relatively long air-paths on the VM side experience common mode optical path length changes to first order and exhibit adequate performance if shielded from turbulence. A larger contribution results from the unbalanced DPML configuration due to global index changes. A particular example of this effect is apparent displacement due relatively quick pressure changes from human traffic, opening and closing of doors, etc. In practice, the effects of this imbalance can be mitigated to acceptable levels by making relatively quick measurements (over a few seconds).

*TABLE 1. Uncertainty budget for the validation metrology*

| Source                            | Value (nm)  |
|-----------------------------------|-------------|
| Environmental effects             | 0.19        |
| Abbè offset (compensated)         | 0.12        |
| Wavelength uncertainty            | 0.03        |
| Slide error motions               | 0.02        |
| Resolution                        | 0.01        |
| Frequency stability               | 0.01        |
| Alignment                         | 0.001       |
| <b>Combined std. uncertainty</b>  | <b>0.22</b> |
| <b>Expanded uncertainty (k=2)</b> | <b>0.44</b> |

### **Uncertainty budget**

The major sources of uncertainty associated with the measurement of the displacement of the SUT relative to the target mirror by the VM are listed in Table 1. The analysis presented in based on the methodology outlined in the ISO Guide to the Expression of Uncertainty In Measurement (GUM) [2]. Practically all the

sources of uncertainty are represented by uniform distributions and most values of influence quantities in the discussion that follows are typically the half-widths of these distributions. The standard uncertainty is explicitly stated in case of exceptions.

Each of the major contributors is discussed in detail below. The uncertainty quoted for each of the contributors is the standard uncertainty.

### **Environmental effects**

This term includes the effects of environmental variables such as pressure, temperature and humidity. The primary contribution results from the effect of the pressure and temperature on the refractive index. The major contribution is due to global temperature and pressure changes during the course of the measurement. This results in an apparent displacement uncertainty of 0.14 nm due to the relatively large deadpath (20 mm) in the interferometer setup and global pressure and temperature variations of 10 mK and 20  $\mu$ m Hg respectively during a typical measurement that lasts a few seconds. The next largest contributions of 0.10 nm results from thermal expansion of the retroreflector mounts, expansion of the target mirror, temperature coefficient of the interferometer and turbulence. Temperature variation of 10 mK is assumed. The remaining contribution of 0.06 nm results from the uncertainty associated with the correction of laser wavelength for the refractive index of air, which in turn arises from the uncertainty associated with the measurement of environmental parameters.

### **Abbè error compensation**

The target mirror is mounted to a linear motor driven crossed-roller linear bearing stage. This stage exhibits two arcseconds and 0.4 arcseconds of pitch ( $\theta_x$ ) and yaw ( $\theta_y$ ) respectively over the scan range. These angular error motions result in an Abbè error due to the offset between the lines of measurement of the SUT and the VM. This offset is in general unknown, but the effects of the pitch and yaw can be compensated for by performing a linear fit to the portion of the measured difference that is correlated to the measured angular error motions. This contribution constitutes a significant source of uncertainty if left uncorrected. After correction, the uncertainty due this contributor is then reduced to the uncertainty in the compensation. Typical Abbè offsets are  $\sim 0.2$  mm and it is estimated that the

uncertainty in the calculation of the offset is 10% or 0.02 mm. In combination with angular error motions of 2 arcseconds, the uncertainty in the compensation contributes 0.12 nm. This includes a contribution due to the uncertainty in the measurement of the angle which results in a contribution of 20 pm.

#### ***Wavelength uncertainty***

The refractive index based correction of wavelength and the associated uncertainty has been described in the section on environmental effects. This correction is based on the vacuum wavelength of the laser which also has an uncertainty associated with it. The nominal uncertainty ( $k=3$ ) in the wavelength of the stabilized HeNe laser used (Zygo ZMI 7712) is 0.16 ppm resulting in a standard uncertainty of  $\sim 0.05$  ppm. This wavelength uncertainty results in a displacement measurement uncertainty of 0.03 nm. Another facet of the wavelength uncertainty is its stability. The long term (24 hour) wavelength stability of this laser head is 0.3 ppb, which results in a 10 pm contribution.

#### ***Slide error motions***

The contributions due to the angular error motions (pitch and yaw) of the slide as a result of the Abbè offset have been discussed above. Other contributions that result from the straightness and roll error motions (rotations about the beam axis) are discussed here. Additional contributions due to pitch and yaw are also discussed here.

Straightness error motions couple into the measurement through two effects: Wedge in the target mirror and out-of-flatness of the target mirror in the region where the beam from the SUT impinges on the target mirror. The two straightness error motions are estimated to be one  $\mu\text{m}$  over the 0.5 mm travel. In conjunction with a wedge of 5 arcseconds in the mirror, this results in a contribution of 0.02 nm. The contributions of pitch and yaw due to two other factors have also been considered and are found to be negligible. These factors are beam shear and optical path length change due to changes in the angular deviation of the return beam. Although the reflectors in this application are retroreflectors, a residual angular deviation of 0.1 arcseconds is assumed which stems from the deviation from 90 degrees of the retroreflector dihedral angle.

#### ***Alignment***

The primary alignment term considered here is the alignment of the DPML beam to the direction of motion. Misalignment causes a cosine error which for this travel range of 0.5 mm is negligibly small ( $\sim 1$  pm) for a relatively coarse (and easily achievable) alignment tolerance of 10 arcsec.

#### ***Periodic errors***

Contributions from periodic (cyclical) errors are conspicuous by their absence in Table 1. Periodic errors result from polarization mixing and are typically observed in most polarization encoded interferometer designs. Contributions due to periodic errors do not appear in this uncertainty analysis because of the unique design of the DPML. The measurement and reference beams are spatially separated (unlike many other interferometer designs) and routed in such a manner through the interferometer that virtually eliminates first-order polarization mixing. This behavior was confirmed experimentally by monitoring the output of the Cyclical Error Correction (CEC) functionality of the measurement boards used in the setup (Zygo ZMI 4004), while rotating the incoming polarization states out of alignment by an amount that would have resulted in a significant periodic error contribution. Virtually no periodic errors were observed.

#### **SUMMARY**

A description of the validation metrology used to validate the performance of a new high-performance displacement sensor has been described along with the results of a detailed uncertainty analysis which shows that the system is capable of displacement measurement with an expanded uncertainty ( $k=2$ ) of  $\sim 0.5$  nm or  $\sim 1$  ppm.

#### **REFERENCES**

- [1] Deck LL, High-performance, multi-channel, fiber-based absolute distance measuring interferometer system. To be published in the Proceedings of the SPIE.
- [2] ISO. Guide to the expression of uncertainty in measurement. 1<sup>st</sup> ed. Geneva: ISO, 1995.